Polymer Chemistry

Accepted Manuscript

ROYAL SOCIETY OF CHEMISTRY

www.rsc.org/polymers

Polymer Chemistry

ARTICLE

Effect of Residue Structure on the Thermal and Thermoresponsive Properties of γ-Substituted Poly(*N*-acryloyl-2-pyrrolidones)†

Received 00th January 20xx,
Accepted 00th January 20xx

DOI: 10.1039/x0xx00000x

www.rsc.org/

R. Bhat,[a] H. Patel,[a] P. -C. Tsai,[b] X. -L. Sun,[a] D. Daoud,[a] R. A. Lalancette,[a] B. Michniak-Kohn[b] and A. Pietrangelo[a*]

We discuss the results of an investigation into the structure/property correlations of γ-substituted poly(*N*-acryloyl-2-pyrrolidone)s, a recently reported class of pyrrolidone-based polymers prepared from pyroglutamic acid, a bio-derived resource. Monomers bearing alkoxy and thiolate substituents were polymerized by reversible addition-fragmentation chain-transfer (RAFT) polymerization with polymer molecular weights and dispersities ($Đ_M$) estimated by gel-permeation chromatography (GPC). Single-crystal X-ray diffraction studies reveal a large degree of steric congestion about the monomer acryl-imide functionality, a topological feature that has residual effects on polymer physicochemical properties when variations to γ-substituent structure are applied. Indeed, glass transition temperature T_g is significantly influenced by both substituent structure (*e.g.*, saturated linear aliphatic *vs* cyclic aliphatic *vs* aromatic) and chemical class with the more thermally stable thiolated polymers possessing lower T_g values than their alkoxy congeners of comparable molecular weight. Regarding solubility, all polymers dissolve in common organic solvents including chloroform, dichloromethane, and tetrahydrofuran while only those bearing methoxyethoxy (**poly(MeOEthONP)**) and tetrahydrofurfuryloxy (**poly(FurONP)**) substituents are soluble in water, a medium where they also exhibit thermoresponsive behavior. Despite the structural similarities among these polymers, a remarkable difference of *ca*. 32°C is observed between their cloud point (CP) temperatures (**poly(MeOEthONP)**, CP = 47°C, **poly(FurONP)**, CP = 15°C) measured during a phase transition that is sensitive to polymer concentration (0.1-1.0 g/L) and chemical environment (*e.g.* deionized water *vs*. phosphate buffered saline (PBS)). Given that both the methoxyethyl thiolate-substituted (**poly(MeOEthSNP**) and substituent-free (**poly(NP)**) polymers are insoluble in aqueous media, we conclude that the observed thermoresponsivity arises from both the topology of the hydrophilic ether-based moiety and identity of the atom (*i.e.* O *vs* S) that tethers the substituent to the lactam scaffold. Finally, cytotoxicity assays were performed on **poly(MeOEthONP)** as its lower critical solution temperature (LCST) is close to that of the human body, an attribute that is desirable for hydrophilic materials used in thermoresponsive drug-delivery platforms. The results of this investigation show that over a concentration range of *ca*. 0.1 - 100 μg/mL, **polyMeOEthONP** formulations are primarily noncytotoxic to both MCF-7 breast cancer cells and human dermal fibroblasts.

Introduction

The extensive use of poly(*N*-vinylpyrrolidone) PVP in the cosmetic, textile, food, and pharmaceutical industries[1] has inspired the creation of new pyrrolidone-based polymers in order to expand their utility towards a wider range of applications. Common strategies employed towards this end include: i) the insertion of spacer groups between the pyrrolidone ring and the polymer backbone[2] and/or ii) the addition of residues to the lactam scaffold,[3] modifications that impart highly desirable properties to these materials including thermoresponsivity in aqueous media.[4] As a result, modified pyrrolidone-based polymers have been used as nanoparticle stabilizers,[5] and complexing agents,[6] and are of considerable interest for use in catalysis[7] and nanoscale drug delivery applications.[8]

While the majority of reports on pyrrolidone-based polymers focus on the synthesis and characterization of polymers bearing α-substituted pyrrolidones,[3,4b] systematic studies on γ-substituted derivatives have received comparatively little attention. Recently, we communicated a facile route to γ-substituted poly(*N*-acryloyl-2-pyrrolidone)s from pyroglutamic acid (PGA), a bio-derived resource.[9] Homopolymers bearing hydrophobic methoxy, ethoxy, and butoxy substituents were prepared by conventional free-radical polymerization and possess a glass transition temperature T_g that is highly sensitive to the length of the

[a] Department of Chemistry, Rutgers University-Newark, 73 Warren Street, Newark, New Jersey 07102, USA
[b] Department of Pharmaceutics, Ernest Mario School of Pharmacy, Rutgers University, 160 Frelinghuysen Road, Piscataway, New Jersey 08854-8022, USA

† Electronic Supplementary Information (ESI) available: Characterization data including ^{1}H and ^{13}C NMR spectra, DSC and TGA thermograms. The X-ray crystallographic file in CIF format has been deposited with the Cambridge Structural Database as file CCDC 1062579. This material can be obtained, free of charge, on application to CCDC, 12 Union Road, Cambridge CB2 1EZ, UK. (fax: +44 1223 336033 or e-mail: deposit@ccdc.cam.ac.uk). See DOI: 10.1039/x0xx00000x

alkoxy substituent. Moreover, modifying the pyrrolidone ring with a methoxyethoxy (*i.e.* $CH_3OCH_2CH_2O$) residue afforded a hydrophilic polymer that exhibits thermoresponsive behavior in deionized water. In addition to these findings, we have also observed that modest adjustments to the pyrrolidone structure have a significant influence on the critical micelle concentration, thermo-induced aggregation, drug loading efficiency, and thermoresponsive drug release of block copolymer micelles bearing γ-substituted poly(*N*-acryloyl-2-pyrrolidone) cores.[8] Taken together, the results of these investigations indicate that the physicochemical properties of these polymers correlate strongly to the molecular architecture of the constituent repeat units. As such, detailed knowledge of structure/property correlations is essential to establishing design criteria if γ-substituted poly(*N*-acryloyl-2-pyrrolidone)s are to have far reaching potential as functional materials, particularly in the field of drug delivery where glass transition temperature,[10] hydrophobic effect,[11] and secondary interactions such as π-π stacking[12] or hydrogen-bonding[13] play a critical role in both drug encapsulation and release.

Herein, we report the details of an investigation into the relationship between γ-substituted poly(*N*-acryloyl-2-pyrrolidone) structure and polymer T_g, T_{dec}, and thermoresponsivity (where applicable). Selection of the monomer substituents was rationalized at two levels that encompass: i) structure (*i.e.* saturated linear/cyclic aliphatic, aryl, ether, and cyclic ether moieties) and ii) chemical classification (*i.e.* alkoxy (RO-) *vs* thiolate (RS-)). RAFT polymerization was employed for this work given the versatility and control of this method.[14] Since pyrrolidone-based polymers are well suited for biomedical applications (due to the pyrrolidone functionality that imparts both coordination ability[15] and biocompatibility[16] to the system), it is anticipated that knowledge gleaned from this work will be used towards the design and application of poly(*N*-acryloyl-2-pyrrolidone)s as potential nanoscale drug-delivery platforms with encapsulating and release capabilities that are made tunable through adjustments to T_g, hydrophobicity, and intermolecular substrate-polymer interactions.

Experimental Section

Materials and Equipment

All reactions were conducted under a dinitrogen atmosphere unless otherwise noted. All reagents were purchased from either Sigma Aldrich or VWR and used as received unless otherwise noted. Deuterated solvents were purchased from Cambridge Isotopes Laboratories, Inc. Phosphate buffered saline (gibco®) was purchased from Life Technologies. Monomers **EthONP**, **BuONP**, **MeOEthONP**,[9] and **NP**[8] were prepared according to literature procedures. Anodic decarboxylation of pyroglutamic acid was conducted in a 1L Chemglass Life Sciences jacketed beaker using a Metrohm USA Inc. AUTOLAB PGSTAT302N potentiostat/galvanostat. Medium extruded graphite plates (*graphitestore.com*) were used as the anode and cathode. ^{1}H NMR spectra were recorded on a Bruker ASCEND 500 MHz spectrometer and calibrated to the residual protonated solvent peaks at δ 7.24 for deuterated chloroform ($CDCl_3$) and δ 5.32 for deuterated dichloromethane (CD_2Cl_2). ^{13}C NMR spectra were calibrated at δ 77.23 for $CDCl_3$ and δ 54.00 for CD_2Cl_2. Turbidimetry experiments were performed on a Cary-100 spectrophotometer equipped with a peltier heated multi-cell holder with a Cary temperature controller and probe. All GC-MS experiments were conducted on an Agilent Technologies HP6890 GC system and 5973A MSD. The standard method involved an initial oven temperature of 70 °C (held for 1 min) followed by a 10 °C min^{-1} ramp to 250 °C. Molecular weights (M_n and M_w) and dispersity ($Đ_M$) were determined by gel permeation chromatography (GPC) using a Malvern Viscotek TDAmax chromatograph with tetrahydrofuran as the mobile phase at 30 °C. The chromatograph was equipped with two PLC mixed columns and one PLD mixed column. Output was detected with a Viscotek TDA 305-055 Tetra Detector Array (PDA+RI+Visc+LALS/RALS) using an eluent flow rate of 1 mL/min and a 60 µL injection loop. Molecular weights were determined from a 10-point calibration curve created using polystyrene standards purchased from Polymer Laboratories. For **poly(NP)**, GPC analysis was performed in DMF/0.01 M LiBr (0.5 mL/min) using a Waters Empower system equipped with a 717plus autosampler, a 1525 binary HPLC pump, a 2487 dual λ absorbance detector, and a 2414 refractive index detector. Two styragel PLC mixed columns (column heater, 50 °C) were used for separation. Molecular weights were determined from a 12-point calibration curve using poly(methyl methacrylate) standards. Differential scanning calorimetry (DSC) was performed on a TA Instruments Discovery differential scanning calorimeter at a scan rate of 10 °C/min. All DSC data were recorded from the second heating scans. Thermal gravimetric analyses were performed on a TA Instruments Discovery thermogravimetric analyzer at a scan rate of 20 °C/min up to 700 °C.

General Procedure for Preparation of γ-substituted 2-pyrrolidones

Method A. A solution of 5-methoxy-2-pyrrolidone **1** (2.0 g, 17 mmol, Scheme 1) in 20 mL of appropriate absolute alcohol was stirred over Amberlyst®15 at 25 °C for 5 h. The solution was filtered over a pad of celite and excess alcohol removed under reduced pressure. The crude products were taken up in a minimum volume of ethyl acetate and recrystallized overnight at *ca*. -28 °C to afford white crystals. *Note: 5-alkoxy-2-pyrrolidones are thermally sensitive and must be stored at ca. 0 °C.*

Method B. Over a period of 15 min, a solution of **1** (2.0 g, 17 mmol) in 5 mL of dichloromethane was added dropwise with constant stirring to a solution of an appropriate absolute alcohol (1.5 molar equiv.) and *p*-toluenesufonic acid (1 mol%) in 5 mL of dichloromethane. After 24 h, the solvent was removed and the residue crystallized by dissolving it in a minimum amount of ethyl acetate and layering with hexanes at -28 °C.

General Procedure for Preparation of γ-substituted *N*-acryloyl-2-pyrrolidones

Over a period of 30 min, n-butyllithium (1.6 M in hexanes, 2.5 mmol) was added dropwise to a solution of 5-alkoxy-2-pyrrolidone (2.5 mmol) in anhydrous THF (*ca*. 70 mL) at -78 °C. At this temperature, the reaction mixture was stirred for 1.5 h followed by the dropwise addition of acryloyl chloride (3.0 mmol). After stirring for an additional 5 h at -78 °C, the reaction was quenched with saturated aqueous NH_4Cl (*ca*. 5 mL) and warmed to room temperature. A drop of *t*-butyl catechol inhibitor solution (15 mM in acetone) was added to the reaction mixture and the solvent removed by reduced pressure. The residue was taken up in ethyl acetate (*ca*. 20 mL) and water (ca. 10 mL) and the solution extracted with ethyl acetate (2x 10 mL). The combined organic phases were washed with saturated $NaHCO_3$ (*ca*. 10 mL) and brine (*ca*. 10 mL), and dried over anhydrous Na_2SO_4. After filtering the mixture, a second drop of inhibitor solution was added to the filtrate and the solvent removed under reduced pressure to afford a yellow opaque oil. The crude product was purified by column chromatography (silica, ethyl acetate/hexanes, 1:1).

General Procedure for Preparation of γ-substituted poly(*N*-acryloyl-2-pyrrolidone)s

Prior to polymerization, all monomers were passed through an alumina plug (using THF as the eluent) to remove inhibitor. Monomer, benzyl benzodithioate (BDTB), and 2,2' azobis(2-methylpropionitrile) (AIBN) (100:1:0.2) were placed in a polymerization tube followed by the addition of anhydrous THF such that monomer concentration was *ca.* 2.0 M. The solution was subjected to freeze-pump-thaw cycles (3x) and the tube backfilled with dry dinitrogen gas before being placed in an oil bath at 70°C for 20 h. The solution was cooled to ambient temperature and added dropwise into rapidly stirring cold hexanes causing a pink solid to precipitate. The polymer was isolated by filtration, dissolved in THF, and reprecipitated in hexanes (2x), followed by drying *in vacuo*. Note: **poly(StSNP)** was precipitated in cold (*ca*. 5 °C) methanol.

***In vitro* Cytotoxicity**

In vitro cytotoxicity studies were conducted using the MCF-7 breast cancer cell line and neonatal human dermal fibroblasts (HDF; Life Technologies). MCF-7 and early passage (before passage 5) of HDF were cultured with Dulbecco's modified Eagle's medium (DMEM; Life Technologies) with 10% fetal bovine serum (Life Technologies), 100 units/mL penicillin (Life Technologies), 100 µg/mL of streptomycin (Life Technologies), and 0.25 µg/mL of amphotericin B (Life Technologies) at 37°C/5% CO_2. Individual wells from 96 well plates were seeded with 5,000 cells/well and incubated for 24 hr prior to experimentation. On the day of the experiment, wells of MCF-7 and HDF cells were treated with 200 µL of DMEM diluted polymer solution ([**poly(MeOEthONP)**] = 1000, 100, 10, 1, 0.1 µg/mL) for 24 h at 37°C. Upon completion, cells were washed with PBS (3x) prior to adding 100 µL of DMEM containing 10% AlamarBlue® reagent (Life Technologies). After incubating at 37°C for 3 h, fluorescence intensity was measured at 590 nm (excitation wavelength, 560 nm) using a microplate reader (Tecan Infinite M200). Cell viability was expressed as a percentage by normalizing the fluorescence intensity of the experimental group relative to DMEM media treated cells; each experimental group was repeated in triplicate.

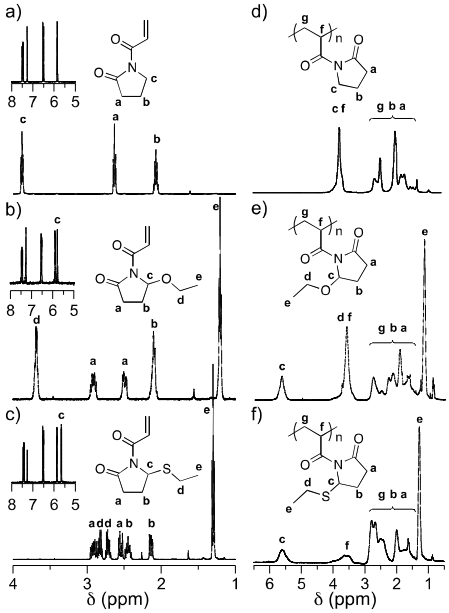

Figure 1. ^{1}H NMR spectra (500 MHz, $CDCl_3$, 25°C) of a) **NP**, b) **EthONP**, c) **EthSNP**, d) **poly(NP)**, e) **poly(EthONP)**, and f) **poly(EthSNP)**.

Results and Discussion

1. Monomer Synthesis

The modularity of PGA-derived *N*-acryloyl-2-pyrrolidones is manifested in the ability to introduce alkoxy and thiolate substituents to the γ-position of the lactam scaffold, a feature that positions the substituent into a vicinity closest to the polymer backbone when compared to α or β-functionalized analogs. All monomers are prepared according to a previously published route that is initiated with the anodic decarboxylation of PGA to 5-methoxy-2-pyrrolidone **1** (Scheme 1).[17] Subsequently, acid-catalyzed alkoxy-exchange with the appropriate residue occurs by either stirring **1** in: i) excess alcohol over Amberlyst 15 (Method A)[18] or ii) dichloromethane in the presence of 1.5 molar equivalents of alcohol and *p*-toluenesulfonic acid (1 mol%) (Method B).[19] The latter is preferred when high-boiling point alcohols (*ca*. > 100°C, *e.g.*, cyclohexanol) are employed due to the thermal sensitivity of γ-substituted pyrrolidones that decompose at elevated temperatures required to remove any residual alcohol. Due to the greater nucleophilicity of thiols over their alcohol congeners, all thiolated pyrrolidones are prepared according to Method A with the exception that only a single molar equivalent of thiol (in THF) is required for near quantitative conversion. All monomers were prepared by deprotonation

with *n*-butyl lithium followed by the addition of *N*-acryloyl chloride. ^{1}H NMR spectra of **EthONP**, **EthSNP**, and *N*-acryloyl-2-pyrrolidone **NP** are shown in Figure 1a-c and share common acryloyl group resonances at *ca*. δ 7.48, 6.51 and 5.84 ppm. The presence of a lactam substituent creates diastereotopic environments across the cyclic scaffold as made evident by both the chemical shifts and complex coupling patterns that are assigned to the *a* and *b* protons of both **EthONP** and **EthSNP** (via 2D NMR (COSY) Spectroscopy, Figures S7 and S8), features that are absent in the spectrum of **NP**. Interestingly, the differences in chemical shift between the diastereotopic *b* protons is more pronounced in **EthSNP** compared to the ethoxy congener, a result that may be attributed to a greater steric demand imposed by the sulfur atom and/or more acute R'-X-R bond angle associated with sulfides (*ca*. 105°).[20] The latter would position the residue closer to the pyrrolidone scaffold generating more distinct diastereotopic environments.

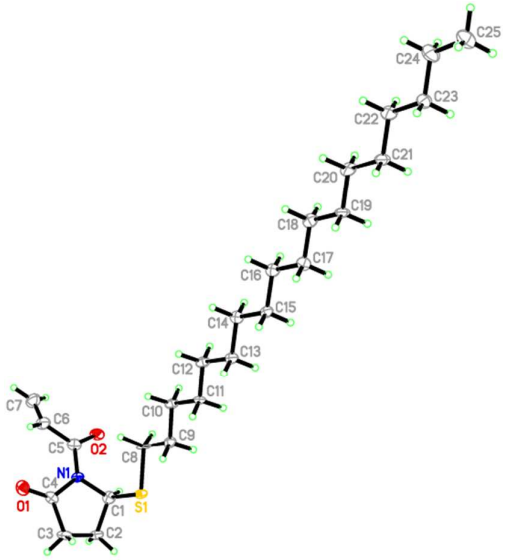

Figure 2. A single molecule representation of the X-ray crystal structure of StSNP as 50% thermal ellipsoids (except H atoms). Key: C = white, N = blue, O = red, S = yellow.

To gain further insight into monomer structure, single-crystal X-ray diffraction studies were performed on **StSNP** (Figure 2), the only monomer that is a solid at room temperature. The γ-substituted *N*-acryloyl-2-pyrrolidone packs into the monoclinic $P2_1/c$ space group with four independent molecules in the asymmetric unit. Crystal packing is stabilized by weak hydrogen-bonding interactions between adjacent acryloyl-pyrrolidone moieties with stearyl chains organized in a non-penetrating bilayer structure. In line with dipole moment and spectroscopic data obtained from *N*-acetyl lactams,[21] **StSNP** adopts an (*E*,*Z*) configuration with Csp^2-Nsp^2 (1.404(8) and 1.394(9) Å) and Csp^2-Osp^2 (1.225(9) and 1.213(9) Å) bond lengths that are consistent with the imide functional group.[22] Indeed, the N atom adopts a trigonal planar geometry with the sum of bond angles around N equal to *ca*. 360°, however the O=C-N-C(O) torsion angles show a deviation from planarity [C(4)-N(1)-C(5)-O(2) = 165.3° and C(5)-N(1)-C(4)-O(1) = -164.9] suggesting that steric hindrance between acryloyl and thiolate groups is causing a twisting of the imide bond. These structural elements in addition to the envelope conformation of the pyrrolidone ring and the proximity of the thiolate residue (R-S-R' bond angle, *ca*. 105.5°) to the acryloyl moiety provide the impetus for tailoring polymer physicochemical properties through only subtle adjustments to both monomer substituent structure and chemical class, a feature that reduces the overall complexity of the system which is highly desirable for creating design rules for nanoparticle drug-delivery platforms.[23]

Scheme 1

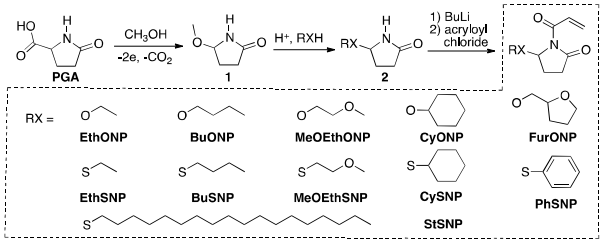

2. Polymer Synthesis and Characterization

All polymers were prepared by RAFT polymerization using a feed molar ratio of $[M]_0$:$[BDTB]_0$:$[AIBN]_0$ = 100:1:0.1 at 70°C for 20 h. GPC traces of the polymers (Figures S35-S45) are typically monomodal with dispersities in the range of 1.4-1.6, values that are considerably lower than those obtained from previously reported poly(*N*-acryloyl-2-pyrrolidone)s prepared by conventional free radical polymerization (*ca*. 2.2-4.0). All ^{1}H NMR spectra (Figures S47-S54) exhibit resonances and integral ratios that are consistent with the targeted polymer structures with common features at *ca*. δ 5.60 and 3.60 assigned to the pyrrolidone γ-hydrogen and -CH_2CH- proton of the polymer backbone respectively (Figure 1d-f, protons *c* and *f*). In the case of alkoxy-functionalized congeners, the latter is buried beneath the OCH_x resonance (Figure 1e, proton *f*) as confirmed through 2D NMR (COSY) studies on small molecule model **3** (Figure S57). In line with our earlier work, all homopolymers are soluble in a variety of organic solvents (*e.g.* dichloromethane, tetrahydrofuran, chloroform, ethylacetate) with only polymers **poly(MeOEthONP)** and **poly(FurONP)** showing limited solubility in water. Interestingly, **poly(NP)** was found to be completely insoluble in water despite possessing the pristine pyrrolidone moieties known to impart water solubility in materials like PVP, indicating that the carbonyl spacer group that comprises the imide functionality has a tremendous influence on the hydrophilicity of the polymer.

Since glass transition temperature can be of particular importance in assessing the processability and performance of a polymeric material, differential scanning calorimetry (DSC) was used to probe polymer thermal transitions as a function of substituent structure. As shown in Figure S58, both **poly(BuONP)** and **poly(BuSNP)** possess lower T_gs than their ethyl-containing analogs (*i.e.* **poly(EthONP)** and **poly(EthSNP)** respectively), results that arise from an increase in polymer

free volume as the linear aliphatic moiety is extended. Moreover, a reduction in T_g is also observed when supplanting a -CH_2- group of the butoxy(thiolate) substituent with an oxygen atom as seen in polymers **poly(MeOEthONP)** and **poly(MeOEthSNP)**.[24] Alternatively, polymers bearing cyclohexyl or phenyl groups (*e.g.*, **poly(CyONP)**, **poly(CySNP)**, and **poly(PhSNP)**) possess the highest T_gs (Figure S58) among the polymers described here, results that are attributed to both the bulky and rigid nature of these substituents that restrict backbone mobility. **Poly(StSNP)** possesses the lowest T_g (*ca*. 30°C) and is the only semi-crystalline polymer with a melt transition temperature T_m of 42°C. A comparative analysis between the alkoxy- and thiolate congeners reveals that irrespective of residue structure, a reduction in T_g is observed (by *ca*. 8-26°C) when sulfur is used in lieu of oxygen. This effect can be attributed to a combination of the larger van der Waals radius of sulfur and/or its poor hydrogen-bond acceptor ability[25] that is expected to weaken cohesive intra- and inter-polymer chain interactions. Finally, TGA thermograms were attained to assess polymer thermal stability. The results clearly show that all alkoxy-functionalized polymers exhibit a multi-step decomposition process (Figures S61-S66) that is more defined than those observed in the thiolate congeners. Moreover, these polymers were all found to possess lower thermal decomposition temperatures (T_{dec}) indicating that γ-substituted poly(*N*-acryloyl-2-pyrrolidone)s bearing thiolate residues are more thermally stable than there alkoxide-bearing analogs regardless of substituent structure.

Table 1. Characterization of Polymers[a)]

Polymer	M_n[b)]	$Đ_M$	T_g (°C)[c)]	T_{dec} (°C)[d)]
poly(NP)	12600[e)]	1.4	120	150
poly(EthONP)	5000	1.4	108	172
poly(EthSNP)	4700	1.5	89	213
poly(ButONP)	6500	1.2	71	186
poly(ButSNP)	6000	1.2	56	320
poly(CyONP)	14800	1.5	129	180
poly(CySNP)	13100	1.4	103	310
poly(PhSNP)	14000	1.6	110	308
poly(MeOEthONP)	9200	1.4	56	170
poly(MeOEthSNP)	10200	1.6	48	317
poly(FurONP	5300	1.5	75	263
poly(StSNP)	16600	1.5	30	311

[a)] [M]:[BDTB]:[AIBN] = 100:1:0.2, [M] = 2.0 M in THF, 70 °C, 20 h. [b)] Determined by GPC (relative to polystyrene in THF). [c)]Glass transition temperature, second heating curve, determined by DSC. [d)] Decomposition temperature, onset, determined by TGA. [e)] Determined by GPC (relative to poly(methylmethacrylate) in DMF).

3. Thermoresponsive Behavior

Endowing thermoresponsive behavior to a polymer can often be achieved by tethering oligoethylene glycol residues to the macromolecular backbone.[26] Using this strategy, we recently reported on the thermoresponsive behavior of **poly(MeOEthONP)** (M_n = 32000, $Đ_M$ = 2.8, prepared by conventional free-radical polymerization) that exhibits a highly reversible and sensitive LCST of *ca*. 42°C in deionized water. In addition, the LCST was adjusted through macromolecular design by simply copolymerizing the ether-functionalized monomer with another bearing hydrophobic methoxy, ethoxy, or butoxy substituents (*e.g.* 31°C, 21°C, and 9°C respectively). As an extension of this work, we sought to analyze the sensitivity of this thermoresponsive behavior in the present study by examining how cloud point (CP) temperature is affected by subtle adjustments to substituent structure, polymer concentration, and chemical environment.

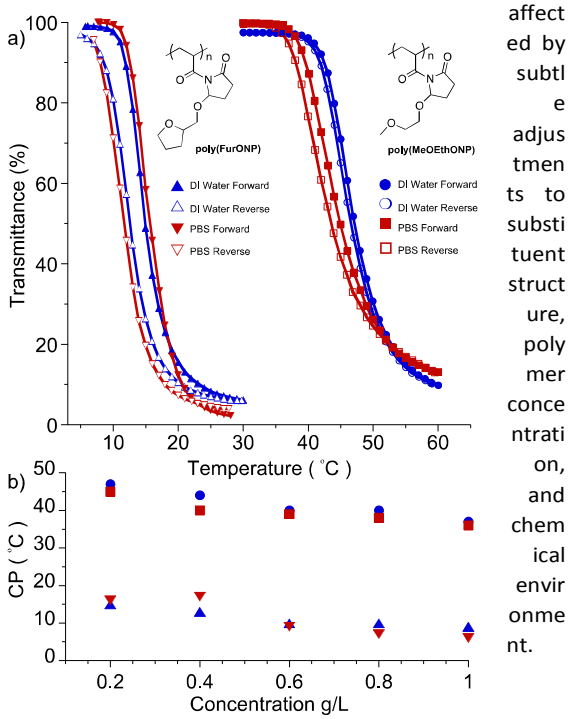

Figure 3. a) Plot of transmittance (%) as a function of temperature in deionized water and PBS solution of **poly(MeOEthONP)** and **poly(FurONP)** (0.2 mg/mL). b) Plot of measured cloud points in deionized water and PBS solution as a function of polymer concentration; **poly(MeOEthONP)**, deionized water, ●; **poly(MeOEthONP)**, PBS solution, ■, **poly(FurONP)**, deionized water, ▲; **poly(FurONP)**, PBS solution, ▼. CP values are measured as the inflection points of the heating cycles.

The thermoresponsive behavior of **poly(MeOEthONP)** and **poly(FurONP)** was measured by turbidimetry and the results illustrated in Figure 3a. Both polymers are completely soluble in deionized water (0.2 mg/mL) resulting in near perfect optical transmittance at 500 nm. Upon approaching the LCST, the solutions turn opaque (a consequence of chain aggregation in solution) with the CP measured as the temperature at which 50% of the original transmittance is lost. In light of the fact that both **poly(NP)** and **poly(MeOEthSNP)** are insoluble in deionized water, the thermoresponsive behavior of **poly(MeOEthONP)** and **poly(FurONP)** must arise from the substituent, specifically, its ether-like topology and alkoxy class. Quite surprisingly, **poly(FurONP)** exhibits a CP (*ca*. 15°C) that is 32°C lower than that of **poly(MeOEthONP)** (*ca*. 47°C) despite the fact that the substituents of the former are structurally related to tetrahydrofurfuryl alcohol which is completely miscible with water.[27] This difference in CP is significant, with its origin a likely combination from both: i) the steric hindrance imposed by the polymer chain on the hydrophilic tetrahydrofurfuryl moieties and ii) the rigid nature of the substituent, contributing factors that are expected to weaken intermolecular polymer/solvent interactions that are responsible for polymer dissolution.[2a] The latter is in line with DSC data and explains why the T_g of **poly(FurONP)** (*ca*. 75°C) is greater than that of **poly(MeOEthONP)** (*ca*. 56°C). Indeed, both polymers redissolve upon cooling below their respective LCST confirming highly reversible thermoresponsive behavior. Moreover, the heating/cooling curve of **poly(MeOEthONP)** exhibits a narrow hysteresis compared to that of **poly(FurONP)**, a phenomenon that is anticipated in more hydrophilic polymers that possess only H-bond donors in the macromolecular structure. Finally, both polymers possess a CP that is concentration dependent (Figure 3b, Table S1), with values that decrease by 10°C and 6°C for **poly(MeOEthONP)** and **poly(FurONP)** respectively over the range of 0.2 - 1.0 mg/mL.

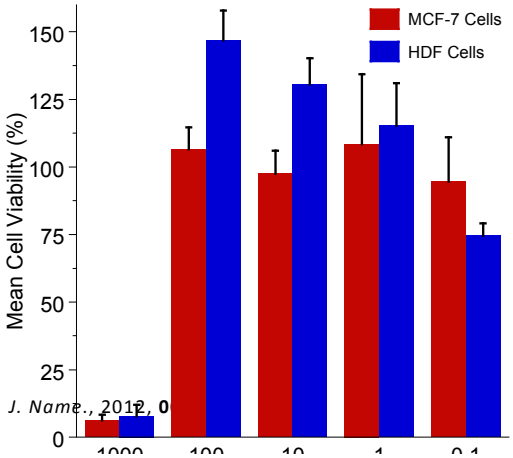

Figure 4. *In vitro* cytotoxicity of **poly(MeOEthONP)** at 37°C. MCF-7 and HDF cells were incubated with polymer for 24h, washed and measured for viability after 3 hr. Data are expressed in mean cell viability (%) with error bars indicating standard deviation. n = 3.

Since the thermoresponsive behavior of (co)polymers can be influenced by the presence of salts,[26a, 28] the CPs of **poly(MeOEthONP)** and **poly(FurONP)** were measured (Figure 3a) in phosphate buffered saline (PBS, [KH_2PO_4] = 1.06 mM, [NaCl] = 155.17 mM, [Na_2HPO_4-$7H_2O$] = 2.97 mM), a solution often used in biological research as a diluent and additive to cell culture media.[29] The results show that at polymer concentrations of 0.2 mg/mL, a subtle salting-out effect was observed for **poly(MeOEthONP)** (*ca*. CP = 45°C), whereas **poly(FurONP)** exhibits a slightly higher CP (*ca*. 16°C) in PBS, consistent with a salting-in effect. As was the case in deionized water, CP values decreased by *ca*. 9°C and 10°C for **poly(MeOEthONP)** and **poly(FurONP)** respectively over the same concentration range (*e.g*. 0.2 - 1.0 mg/mL, Figure 3b, Table S1). Taken, together, the results suggest that the thermoresponsivity of these systems is relatively insensitive to changes in environmental conditions with CPs varying only a few degrees between deionized water and PBS formulations.

4. In Vitro Cytotoxicity

Materials that exhibit thermoresponsivity in aqueous media at temperatures approaching that of the human body (*ca*. 38°C) are highly desirable for biotechnology applications.[30] On this bases, the cytotoxicity of **poly(MeOEthONP)** was evaluated at 37°C using human dermal fibroblasts (HDF) and MCF-7 breast cancer cells. The results of this investigation are plotted in Figure 4 and indicate that **poly(MeOEthONP)** exhibits high cell viability in the concentration range of 0.1 - 100 μg/mL, a desirable attribute for drug delivery platforms that rely on a thermal stimulus to release a therapeutic payload to an affected area without compromising the health of non-targeted cells.

Conclusions

Structure/property correlations on γ-substituted poly(*N*-acryloyl-2-pyrrolidone)s have been investigated. When compared against their alkoxy congeners of comparable molecular weight, the thiolated polymers possess higher thermal stability and lower T_gs regardless of substituent structure. The results also show that glass transition temperature can be modified over a broad temperature range by making subtle adjustments to the substituent structure, a feature that could be attributed to steric congestion between the pyrrolidone γ-substituent and polymer backbone as inferred from a single crystal x-ray diffraction study on monomer **StSNP**. Among the systems studied in this report, only **poly(MeOEthONP)** and **poly(FurONP)** are soluble in deionized water exhibiting a cloud point at 47°C and 15°C (0.2

mg/mL) respectively, thermoresponsive behavior that is also concentration dependent over the range of 0.2-1.0 mg/mL. At fixed polymer concentrations, the CP values in deionized water are comparable to those measured in PBS solution indicating that the salts (present in the latter) have little effect on the thermoresponsivity. Moreover, polymers **poly(NP)** and **poly(MeOEthSNP)** were found to be insoluble in aqueous media indicating that the thermoresponsive behavior of **poly(FurONP)** and **poly(MeOEthONP)** arises solely from the ether moiety and the oxygen atom that tethers it to the lactam ring. Finally, *in vitro* cytotoxicity studies using both MCF-7 and HDF cells revealed that **poly(MeOEthONP)** is largely noncytotoxic over the polymer concentration range of 0.1-100 μg/mL. The information obtained from this study provides evidence for the potential utility of γ-substituted poly(*N*-acryloyl-2-pyrrolidone)s as they can be tailored to adjust: i) hydrophobic or hydrophilic character, ii) thermoresponsivity, iii) hydrogen-bonding (alkoxy *vs* thiolate substituents) / π-π stacking (cyclohexyl vs phenyl moieties) capability, and iv) T_g, without complex modifications to the macromolecular scaffold. Systems such as these are highly desirable for biomedical applications, particularly as drug delivery platforms that are designed to load and release therapeutic payloads in a controlled manner. Compelled by the negligible toxicity of **poly(MeOEthONP)**, efforts to prepare block copolymer micelles with **poly(MeOEthONP)** coronae and γ-substituted poly(*N*-acryloyl-2-pyrrolidone)s cores are currently underway to examine how both substituent structure and chemical class influence the physicochemical properties, drug-loading efficiency, and thermoresponsive release among this novel class of pyrroldione-based polymer.

Acknowledgements

The authors thank Rutgers University (including the Busch Biomedical Grant program) for financial support and the NSF for funds used to purchase the Bruker ASCEND 500 MHz spectrometer (NSF MRI 1229030).

Notes and references

1 (*a*) F. Fisher and S. Bauer, *Chem. Unserer Zeit* 2009, **43**, 376; (*b*) F. Haaf, A. Sanner and F. Straub, *Polym. J.,* 1985, **17**, 143; (*c*) A. J. M. D'Souza, R. L. Schowen and E. M. Topp, *J. Controlled Release,* 2004, **94**, 91.

2 (a) P. Liu, L. Xiang, Q. Tan, H. Tang and H. Zhang, *Polym. Chem.*, 2013**, 4**, 1068; (*b*) I. Atobe, T. Takata and T. Endo, *Macromolecules,* 1994, **27**, 193; (*c*) J. Sun, Y. Peng, Y. Chen, Y. Liu, J. Deng, L. Lu, and Y. Cai, *Macromolecules,* 2010, **43**, 4041.

3 G. -T. Chen, C. -H. Wang, J. -G. Zhang, J. Wang, R. Zhang, F. -S. Du, N. Yan, Y. Kou and Z. -C. Li, *Macromolecules,* 2010, **43**, 9972.

4 (*a*) H. Lai, G. Chen, P. Wu and Z. Li, *Soft Matter,* 2012, **8**, 2662; (*b*) T. Trellenkamp and H. Ritter, *Macromol. Rapid Commun.,* 2009, **30**, 1736; (*c*) J. Deng, Y. Shi, Y. Peng, L. Lu, and Y. Cai, *Macromolecules,* 2008, **41**, 3007; (*d*) G. M. Iskander, L. E. Baker, D. E. Wiley and T. P. Davis, *Polymer,* 1998, **39**, 4165; (*e*) X. Savelyeva and M. Marić, *J. Polym. Sci. Part A: Polym. Chem.,* 2014, **52**, 2011.

5 (*a*) B. V. Popp, D. H. Miles, J. A. Smith, I. M. Fong, M. Pasquali and Z. Ball, *J. Polym. Sci. Part A: Polym. Chem.,* 2015*,* **53***,* 337; (*b*) N. Yan, J. Zhang, Y. Tong, S. Yao, C. Xiao, Z. Li and Y. Kou, *Chem. Commun.*, 2009, 4423.

6 T. Trellenkamp and H. Ritter. *Macromolecules,* 2010, **43**, 5538.

7 (*a*) J. Zhang, Y. Yuan, K. J. Kilpin, Y. Kou, P. J. Dyson, and N. J. Yan, *J. Mol. Catal. A: Chem.*, 2013, **371**, 29; (*b*) N. Yan, J. Zhang, Y. Yuan, G. -T. Chen, P. J. Dyson, Z. -C. Li, and Y. *Chem. Commun*., 2010, **46**, 1631.

8 X. -L. Sun, P. -C. Tsai, R. Bhat, E. M. Bonder, B. Michniak-Kohn and A. Pietrangelo, *J. Mater. Chem. B*, 2015, **3**, 814.

9 R. Bhat and A. Pietrangelo, *Macromol. Rapid Commun.,* 2013, **34**, 447.

10 (*a*) D. A. Norris, N. Puri and P. J. Sinko, *Adv. Drug. Deliv. Rev*., 1998, **34**, 135; (*b*) V. Karavelidis, D. Giliopoulos, E. Karavas and D. Bikiaris, *Eur. J. Pharm. Sci.,* 2010, **41**, 636; (*c*) M. O. Omelczuk and J. W. McGinity, *Pharm. Res.,* 1992, **9**, 26.

11 (*a*) D. Attwood, C. Booth, S. G. Yeates, C. Chaibundit and N. Ricardo, *Int. J. Pharm.,* 2007, **345**, 35; (*b*) S. W. Kim, Y. Z. Shi, J. Y. Kim, K. N. Park and J. X. Cheng, *Expert Opin. Drug. Deliv.* 2010, **7**, 49.

12 (*a*) K. M. Huh, H. S. Min, S. C. Lee, H. J. Lee, S. Kim and K. Park, *J. Controlled Release*, 2008, **126**, 122; (*b*) K. M. Huh, S. C. Y. W. Cho, J. Lee, J. H. Jeong and K. Park, *J. Controlled Release*, 2005, **101**, 59.

13 L. L. Chang, L. D. Deng, W. W. Wang, Z. S. Lv, F. Q.; Hu, A. J. Dong, and J. H. Zhang, *Biomacromolecules,* 2012, **13**, 3301.

14 (*a*) C. Boyer, V. Bulmus, T. P. Davis, V. Ladmiral, J. Liu and S. Perrier, *Chem. Rev.* 2009, **109**, 5402; (*b*) G. Moad, E. Rizzardo and S. H. Thang, *Chem. Asian J.* 2013, **8**, 1634.

15 (*a*) H. Einaga and M. Harada, *Langmuir*, 2005, **21**, 2578; H. Tsunoyama, H. Sakurai, Y. Negishi and T. Tsukuda, *J. Am. Chem. Soc.* 2005, 127, 9374; (*b*) J. M. Smith, J. Meadows, and P. A. Williams, *Langmuir,* 1996, **12**, 3773.

16 B. V. Robinson, F. M. Sullivan, J. F. Borzelleca and S. L. Schwartz, *PVP: A Critical Review of the Kinetics and*

Toxicology of Polyvinylpyrrolidone (Povidone); Lewis Publishers: Chelsea, MI, 1990.
17 (*a*) T. Iwasaki, H. Horikawa, K. Matsumoto and M. Miyoshi, *J. Org. Chem*. 1979, **44**, 1552; (*b*) T. Iwasaki, H. Horikawa, K. Matsumoto and M. Miyoshi, *J. Org. Chem*., 1977, **42**, 2419.
18 E. Toja, C. Gorini, C. Zirotti, F. Barzaghi, and G. Galliani, *Eur. J. Med. Chem*., 1991, **26**, 415.
19 D. Savoia, V. Concialini, S. Roffia and L. Tarsi, *J. Org. Chem.,* 1991, **56**, 1822.
20 S. Oae, *Organic Sulfur Chemistry: Structure and Mechanism*; Doi, J. T. *Ed*.; CRC Press: Boca Raton, FL, 1992, p.6.
21 C. M. Lee and W. D. Kumler, W. D. *J. Am. Chem. Soc.,* 1962, **84**, 565.
22 F. H. Allen, O. Kennard, D. G. Watson, L. Brammer, A. G. Orpen and R. Taylor, *J. Chem. Soc., Perkin Trans. 2* 1987, S1.; A. Saeed, M. Erben and M. Bolte, *J. Org. Chem.* 2012, **77**, 4688.
23 C. M. Dawidczyk, C. Kim, J. H. Park, L. M. Russell, K. H. Lee, M. G. Pomper, and P. C. Searson, *J. Controlled Release*, 2014, **187**, 133.
24 [24] This can be attributed to an enhancement in substituent flexibility that arises when supplanting CH_2 groups in linear aliphatic chains with oxygen atoms. An increase in substituent flexibility can facilitate side-chain bond rotation and reduce polymer T_g. *See* (a) M. Szycher, *Szycher's Handbook of Polyurethanes,* First Edition; CRC Press: Boca Raton, FL, 1999, p. 696 and (b) P. C. Painter and M. M. Coleman, *Fundamentals of Polymer Science: An Introductory Text, Second Edition*; Technomic Publishing Co. Inc. Lancaster, PA, 1997, p. 301.
25 (*a*) J. A. Platts, S. T. Howard and B. R. F. Bracke, *J. Am. Chem. Soc.,* 1996, **118**, 2726; (*b*) S. Bhattacharyya, A. Bhatacherjee, P. R. Shirhatti and S. Wategaonkar, *J. Phys. Chem. A*., 2013, **117**, 8238; (*c*) H. S. Biswal and S. Wategaonkar, *J. Chem. Phys*., 2011, **135**, 134306-1.
26 (*a*) J. -F. Lutz, Ö. Akdemir and A. Hoth, *J. Am. Chem. Soc.,* 2006, **128**, 13046; (*b*) J. -F. Lutz and A. Hoth, *Macromolecules* 2006, **39**, 893.
27 *The Merck Index: An Encyclopedia of Chemicals and Drugs*, 8th ed.; P. G. Stecher, M. Windholz, D. S. Leahy, D. M. Bolton, and L. G. Eaton, Eds.; Merck & Co.; Rahway, N.J., 1968; p 1027.
28 (*a*) K. Van Durme, H. Rahier and B. Van Mele, *Macromolecules,* 2005, **38**, 10155; (*b*) Y. Zhang, S. Furyk, D. E. Bergbreiter and P. S. Cremer, *J. Am. Chem. Soc.* 2005, **127**, 14505. (c) Yuan, W. and Wang, J. *RSC Advances*, 2014, **4**, 38855-38858. (d) Lutz, J. -F., Weichenhan, K., Akdemir, Ö. and Hoth, A., *Macromolecules*, 2007, **40**, 2403-2508. e) Iizawa, T., Yamamoto, D., Gotoh, T. and Sakohara, S., *Polymer*, 2012, **53**, 3417-3420.
29 M. Lichtenauer, S. Nickl, K. Hoetzenecker, A. Mangold, B. Moser, M. Zimmermann, S. Hacker, T. Niederpold, A. Mitterbauer and H. J. Ankersmit, *Lab Med.*, 2009, **40**, 290.
30 H. Wei. S. -X. Cheng, X. -Z. Zhang and R. -X. Zhuo, *Prog. Poly. Sci.* **2009**, *34*, 893.

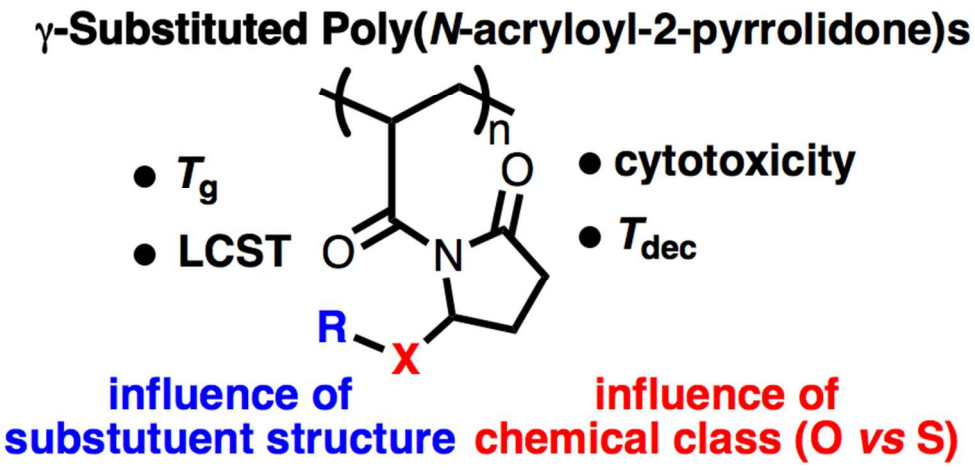

323x149mm (72 x 72 DPI)